Carrier capture and relaxation in Stranski-Krastanow $In_xGa_{1-x}As/GaAs(311)B$ quantum dots

C. Lobo
Department of Electronic Materials Engineering, Research School of Physical Sciences and Engineering, Australian National University, Canberra ACT 0200, Australia

N. Perret and D. Morris
Departement de Physique, Universite de Sherbrooke, Sherbrooke J1K 2R1, Quebec, Canada

J. Zou and D. J. H. Cockayne
Australian Key Centre for Microscopy and Microanalysis, University of Sydney, Sydney 2006, NSW Australia

M. B. Johnston and M. Gal
School of Physics, University of New South Wales, Sydney 2052, NSW Australia

R. Leon
Jet Propulsion Laboratory, California Institute of Technology, Pasadena, California 91109
(Received 29 November 1999; revised manuscript received 25 February 2000)

We have investigated the structure and optical properties of $In_{0.6}Ga_{0.4}As/GaAs(311)B$ quantum dots (QD's) formed by the Stranski-Krastanow growth mode during metal-organic chemical-vapor deposition. We find that $(311)B$ QD structures display a higher energy QD luminescence emission and a stronger wetting-layer emission than (100) QD's of similar diameter and density. Temperature-dependent photoluminescence (PL) measurements reveal shallow QD confinement energies and strong interaction between neighboring quantum dots. Longer PL rise times of the ground-state emission of $(311)B$ QD's compared to (100) QD's are ascribed to the effect of differing numbers, energies, and level spacings of QD confined states on intersublevel relaxation mechanisms at low-carrier excitation densities.

I. INTRODUCTION

High-density InGaAs/GaAs quantum dot (QD) structures have numerous potential device applications in infrared lasers, photodetectors, and optical memory devices. The majority of these structures are grown on the (100) surface orientation using the Stranski-Krastanow mode of self-assembled QD growth. Quantum dot structures formed on the $(311)B$ GaAs surface have also been of great interest due to their size uniformity, and the ability to achieve positional ordering into high-density, two-dimensional arrays utilizing a unique self-organizing growth mode in metal-organic vapor phase epitaxy.[1,2] A tendency towards positional ordering has also been observed in low indium content InGaAs/GaAs$(311)B$ QD's grown by the Stranski-Krastanow mode in H-irradiated molecular-beam epitaxy (MBE) and gas-source MBE. However, due to the low indium content of these QD's, the dots are either very large,[3] or metastable under annealing at the growth temperature,[4] limiting the usefulness of these arrays in device applications.

Here we have studied the electronic and optical properties of randomly distributed Stranski-Krastanow InGaAs/GaAs$(311)B$ quantum dots by temperature-dependent and time-resolved photoluminescence (TRPL) measurements. We find that compared to InGaAs/GaAs(100) QD's grown under equivalent conditions, $(311)B$ QD's display a higher QD emission energy, strong luminescence emission from the wetting layer, and slower carrier transfer times under low excitation. These results are interpreted in terms of the effect of differing numbers, energies, and level spacings of QD states on the relaxation mechanisms under low-carrier excitation densities.

II. EXPERIMENTAL PROCEDURE

InGaAs/GaAs$(311)B$ QD's were grown by metal-organic chemical-vapor deposition in a horizontal reactor cell operating at 76 Torr. Trimethylgallium, trimethylindium, and arsine were used as precursors. Growth of a 50 nm GaAs buffer layer at 650 °C was followed by deposition of 1.5 nm InGaAs with a nominal indium mole fraction of 0.6. The growth temperature and growth rate during QD formation were 550 °C and 0.5 ML/s, respectively. The QD's used for photoluminescence measurements were buried with a 100 nm GaAs capping layer deposited while the temperature was raised gradually to 650 °C.

Determination of island sizes and densities in the capped samples used for photoluminescence measurements was carried out by plan-view transmission electron microscopy (TEM) using a Philips CM12 operating at 120 keV. Island concentrations were also estimated from atomic force microscopy (AFM) images of uncapped samples grown under equivalent conditions to the capped samples used for PL. AFM imaging was conducted in contact mode using a Digital Instruments Nanoscope III AFM and standard silicon nitride tips.

Temperature-dependent PL measurements were obtained using a green He-Ne laser emitting at 543 nm. The signal

 ©2000 The American Physical Society

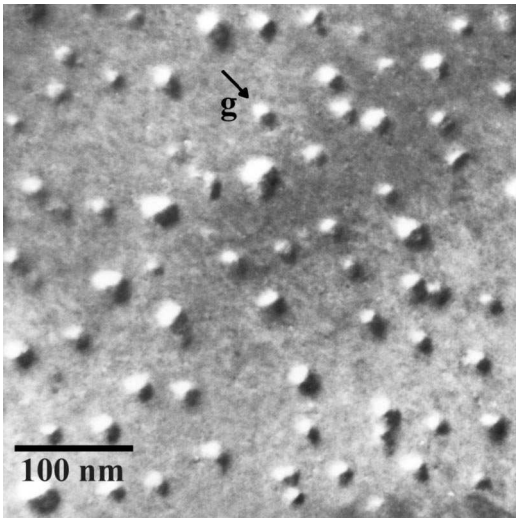

FIG. 1. Dark field plan-view TEM micrograph of buried $In_{0.6}Ga_{0.4}As/GaAs(311)B$ QD's. The dark/light contrast is obtained under two-beam dynamical diffraction conditions [diffraction vector $g=(02\bar{2})$]. Average sizes and densities of these buried QD's are given in the text.

was dispersed by a 0.25-m single-grating monochromator and collected using a silicon charge coupled device. Time-resolved photoluminescence measurements were performed at 77 K. A mode-locking Ti:sapphire laser (80 fs, 82 MHz, 812 nm) was used for excitation and an upconversion technique with subpicosecond temporal resolution and a GaAs photomultiplier tube were used for signal detection. Power excitation densities varied in the range 2 to 200 W/cm^2.

Figure 1 shows a dark field plan-view TEM image [diffraction vector $g=(02\bar{2})$] of the capped (311)*B* QD's formed by the Stranski-Krastanow growth mode. The high-nominal indium content and consequent small sizes of these QD's relative to those examined in previous studies,[3] result in a disordered dot array. Analysis of dark field TEM images taken using different diffraction vectors gives dot diameters of the order of (25 ± 5) nm. The average dot density is 3×10^{10} cm^{-2}, determined both from plan-view TEM images of capped samples and AFM images of uncapped samples grown under equivalent conditions.[5]

III. TEMPERATURE-DEPENDENT PL

Low-temperature (10 K) continuous-wave (cw) PL spectra from the (311)*B* InGaAs/GaAs QD's and a (100) reference sample grown under similar conditions, are displayed in Fig. 2. The average dot diameter and density in the (100) QD sample are (25 ± 5) nm and 2.5×10^{10} cm^{-2}, respectively. The QD PL emission of the (311)*B* sample is blueshifted by 140 meV relative to the (100) QD's, although the average diameter of QD's in both samples is similar. This blueshifting of the (311)*B* QD emission can be attributed to a differing amount of strain in the structure and/or stronger confinement in the growth direction. Aspect ratios [ratio of island height (h) to diameter (d)] of uncapped (311)*B* quantum dots have been determined by analysis of AFM images and found to be smaller than for (100) quantum dots grown under similar conditions ($h/d=1/8$ and 1/6, respectively). The

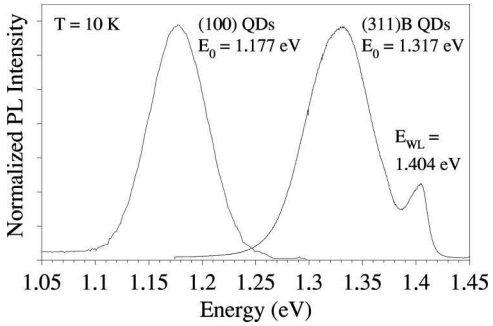

FIG. 2. Low-temperature PL spectra of $In_{0.6}Ga_{0.4}As/GaAs$ QD's grown on (311)*B* and (100) GaAs under similar conditions.

higher energy (311)*B* QD emission may also be accounted for by a differing local ternary composition in the QD's. Indium segregation and enrichment of InGaAs/GaAs(100) QD's has been found to result in QD's with average indium compositions 30%–45% higher than that of the deposited film.[6] Stress-induced indium enrichment of quantum dots formed from $In_xGa_{1-x}As$ films has been predicted to reduce the nucleation barrier for islanding, with a resultant island composition that depends critically on the island shape and fractional elastic relaxation of the island relative to the planar layer.[7] Indium enrichment effects have not been determined in InGaAs/GaAs(311)*B* QD's, but may well be reduced relative to (100) QD's, which would result in a higher gallium content in (311)*B* QD's compared to (100) QD's of similar diameter. Surface segregation of indium, which acts in the opposite direction to stress-induced enrichment and reduces the indium composition at the core of the quantum dots, must also be considered.[7,8]

The InGaAs/GaAs(311)*B* spectrum displays a strong wetting layer (WL) PL peak at 1.404 eV, which persists up to 70 K. Emission from the InGaAs WL is not observed in cw PL from high-density InGaAs/GaAs(100) QD's except at very low temperature (<20 K) or very high-excitation power densities.[9,10] The WL emission energies in these (100) and (311)*B* QD structures differ ($E_{WL}^{(100)}=1.30$ eV, $E_{WL}^{(311)B}=1.40$ eV at 10 K). This indicates that the WL in (311)*B* QD's is narrower than in (100) QD's and/or has a higher gallium content. The latter would result from increased indium surface segregation in (311) structures, which is known to produce blueshifts of transition energies in InGaAs/GaAs(311) quantum wells.[11–13]

The temperature dependence of the PL emission from the (311)*B* QD's was studied over the temperature range 10–200 K. Between 10 and 70 K, emission from the QD ground state and the wetting layer is observed (Fig. 2). For $T\geqslant80$ K, PL emission from the WL is quenched due to thermal activation of carriers to the GaAs barrier, and slight asymmetric broadening of the high-energy side of the (311)*B* QD PL spectrum becomes evident (see Fig. 3). The intensity of this high-energy shoulder relative to that of the ground-state QD emission increases with increasing temperature. This broadening of the PL spectrum is ascribed to filling of the first QD excited state. Due to the large degree of inhomogeneous broadening [full width at half maximum (FWHM)$\approx$60–70 meV], the QD ground and excited state(s) cannot be resolved. However, good fits to the PL spectra can be obtained using two Gaussians with an identical inhomo-

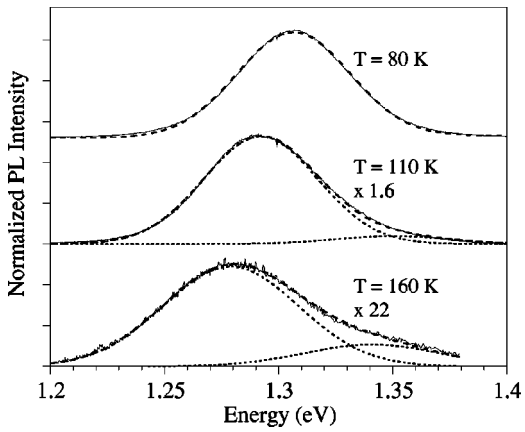

FIG. 3. PL spectra of $In_{0.6}Ga_{0.4}As/GaAs(311)B$ QD's at temperatures between 80 and 160 K. The 80 K PL spectrum can be modeled by a single Gaussian, while for $T>80$ K, two Gaussians with identical inhomogeneous broadening factors and intersublevel separation of approximately 60 meV are required to fit the spectra.

geneous broadening factor ($\Gamma = 1/2$ FWHM) and an intersublevel separation of approximately 60 meV. This intersublevel spacing is larger than that observed for high-density (100) QD's (45–50 meV),[10] which may be a consequence of greater confinement in the growth direction as evidenced by the reduced island aspect ratios in (311)*B* QD structures.

A. QD emission

Figure 4(a) shows the redshift $[E_{max}(T)-E_{max}(10\ K)]$ of the ground-state QD PL emission as a function of temperature. For both (311)*B* QD's and (100) QD's of comparable density, the magnitude of this redshift is significantly greater than that of the InGaAs free exciton emission[14] (dashed line). However, unlike the (100) dots, the (311)*B* QD emission displays a significant deviation from the temperature dependence of the bulk InGaAs emission even at low temperature (40–50 K). The amount of the (311)*B* QD PL redshift is also greater than that for (100) QD's across the whole temperature range. The variation in the inhomogeneously broadened linewidth of the ground-state QD emission from (311)*B* and high-density (100) QD's is shown in Fig. 4(b). Both types of QD's show similar behavior, although the (311)*B* QD's display a much greater variation of FWHM with temperature than the (100) QD's (15 meV compared to 8 meV).

These dependencies of the energy shift and FWHM of the QD PL peak on temperature are attributed to the effects of thermal activation transfer of carriers between neighboring QD's. For the (100) QD's, there is no significant thermal emission of carriers out of the QD's at low temperatures (below $\approx$100 K). The PL energy position and FWHM of the QD emission therefore remain constant. Above 100 K, carrier thermal emission out of the smaller QD's in the ensemble and recapture by neighboring QD's with deeper confining potentials becomes important. This behavior explains the simultaneous redshifting and narrowing of the PL peak. At higher temperatures (above 150 K) the FWHM increases and the rate of redshift decreases as thermal emission of carriers out of the larger QD's in the ensemble becomes significant.[15] These same behaviors are shifted to lower temperatures for the (311)*B* QD's, reflecting increased effects of strain interactions[10] and thermally activated carrier transfer[15] between neighboring QD's.

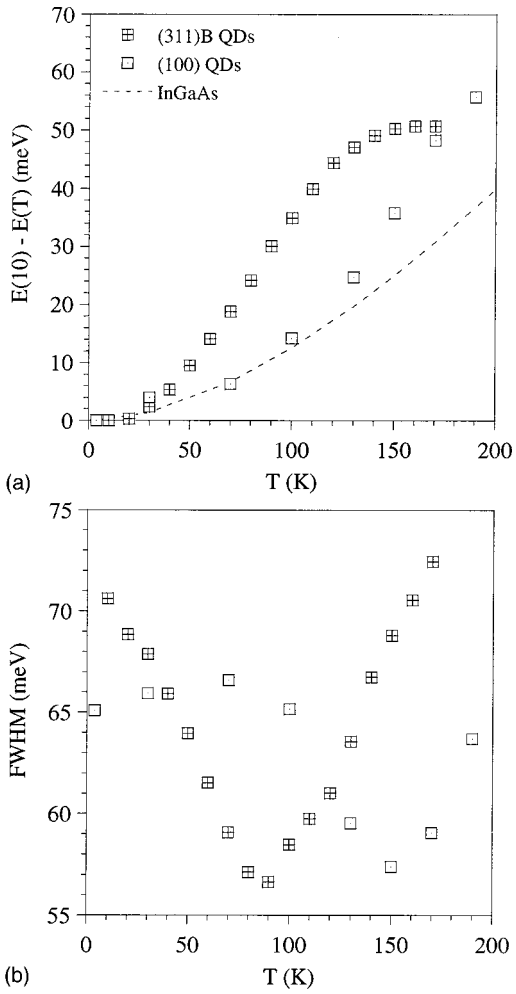

FIG. 4. Temperature dependence of the (a) PL redshift and (b) inhomogeneous linewidth broadening (FWHM) of the emission from (311)*B* and (100) QD's. The dashed line represents the PL redshift of the InGaAs free exciton emission.

The PL emission from (311)*B* dots is also found to quench at lower temperature than for (100) QD's of similar size and density. The activation energy for PL quenching extracted from the Arrhenius plot shown in Fig. 5 is only 80 meV, which is equivalent to the energy difference between the QD peak and the WL emission ($E_{QD}-E_{WL}=87$ meV). Hence the mechanism of QD PL quenching is ascribed to thermal emission of carriers into the InGaAs WL. The activation energy for PL quenching is substantially lower than for high-density (100) QD's[16,17] due to the shallower confinement energy.

B. WL emission

As discussed above, strong emission from the InGaAs WL is only observed in cw PL from InGaAs/GaAs(100) QD's at low dot densities. The strong emission from the InGaAs WL underlying the (311)*B* QD's permitted a comparative study of the temperature dependence of the WL PL emission energy and linewidth in (100) and (311)*B* QD

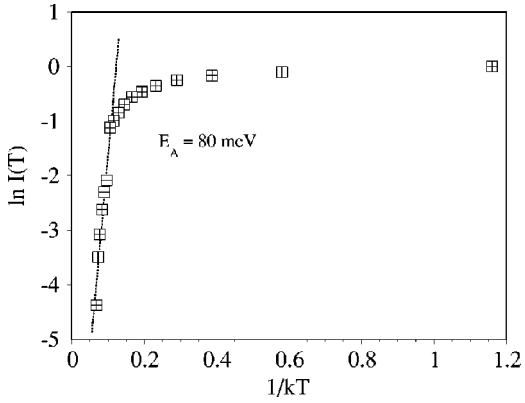

FIG. 5. Arrhenius plot of the PL intensity from $In_{0.6}Ga_{0.4}As/GaAs(311)B$ QD's. The activation energy E_A extracted from this Arrhenius plot approximates the energy difference between the QD emission and that of the InGaAs WL.

structures. This data is displayed in Fig. 6. Two low-density (100) QD structures were studied: one with a QD density of 3.7×10^8 cm^{-2} (sample *A*) and the other with a QD density of 7×10^8 cm^{-2} (sample *B*).[15] Quantum dots in both (100) samples have an average diameter of 25±5 nm. For both

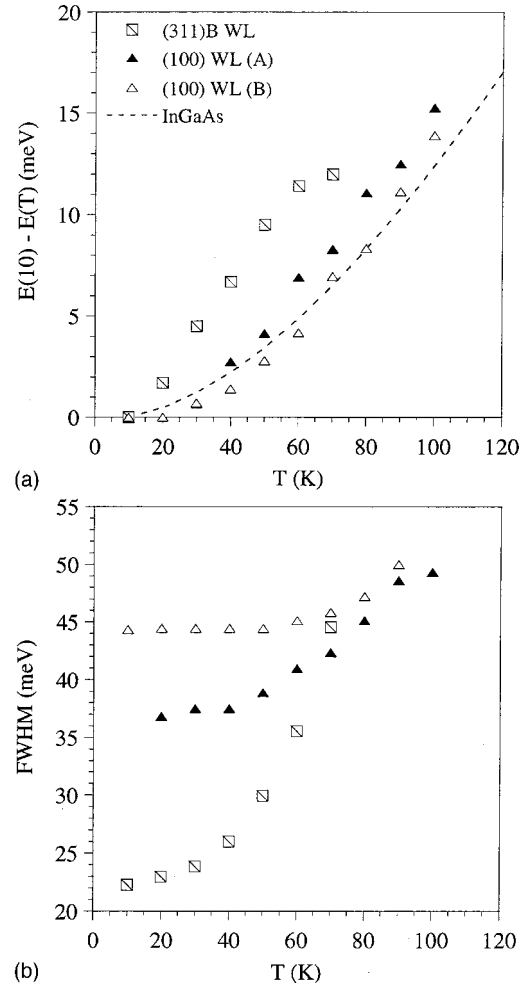

FIG. 6. Temperature dependence of the (a) PL redshift and (b) inhomogeneous linewidth broadening (FWHM) of the emission from the InGaAs WL in (311)*B* and (100) QD samples. The dashed line represents the PL redshift of the InGaAs free exciton emission.

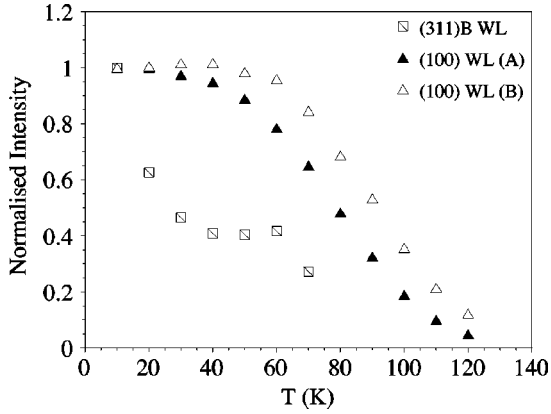

FIG. 7. Normalized PL intensity of the WL emission as a function of temperature for (311)*B* QD's compared to that of two low-density (100) QD structures.

low-density (100) QD structures, the WL emission energy shifts with that of the InGaAs free exciton emission with increasing temperature [see Fig. 6(a)]. The FWHM of the WL emission in these low-density (100) QD samples increases gradually with increasing temperature as shown in Fig. 6(b). This behavior is attributed to the effects of multiphonon scattering. In contrast, the WL emission in (311)*B* QD structures displays an above-bandgap PL redshift [Fig. 6(a)] and a much more pronounced increase of the luminescence linewidth [Fig. 6(b)] with increasing temperature. These behaviors are attributed to the effects of carrier redistribution from weakly to strongly confined regions of the WL as the temperature increases.

Interestingly, the intensity of the PL emission from the InGaAs WL underlying the (311)*B* QD's does not decrease according to an Arrhenius law with increasing temperature (see Fig. 7). Instead, the WL emission shows an increase in intensity that offsets the decrease of the PL intensity resulting from thermal emission of carriers to the barrier. This behavior contrasts with that of the WL in low-density (100) QD samples (Fig. 7) and with that of the (311)*B* QD emission (Fig. 5), which both display Arrhenius dependencies on temperature.

IV. TIME-RESOLVED PL

Carrier capture and relaxation in InGaAs/GaAs(311)*B* QD structures was further investigated by TRPL using excitation above the GaAs bandgap. Figure 8 shows TRPL spectra from the (311)*B* QD's taken at different delays after the pulsed laser excitation at $T=77$ K. Significant state filling effects are observed even at this low-excitation density ($P=10$ W/cm^2). The blueshift of the QD PL band between 20 and ≈500 ps is due to filling of excited states.[18] Note that the QD transitions associated with ground and excited states are not resolved due to the large degree of inhomogeneous broadening. Similarly, the WL emission (observed at 1.404 eV in cw PL and in TRPL under high-excitation densities) cannot be resolved from the QD excited states at low-excitation density. The redshift of the PL band at longer delay times is attributed to replenishing of ground-state carriers from the excited states of the QD's. Carrier thermal emission from high-energy QD's and retrapping by lower-

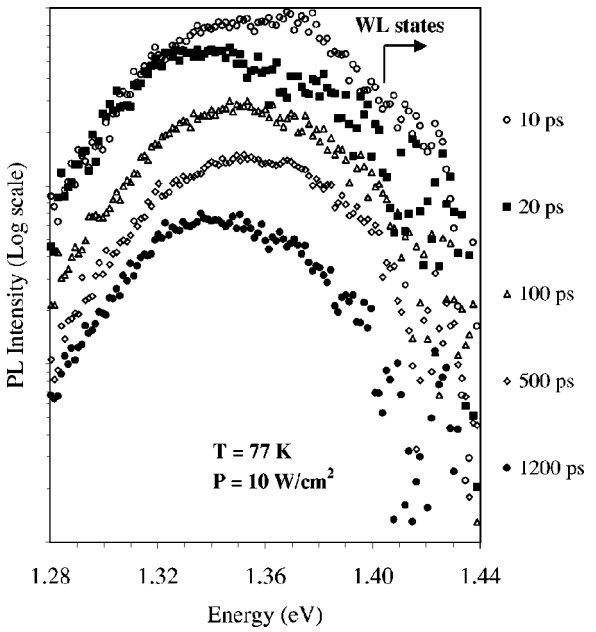

FIG. 8. Transient PL spectra from (311)*B* QD's at various delays after pulsed excitation for an excitation density of 10 W/cm^2.

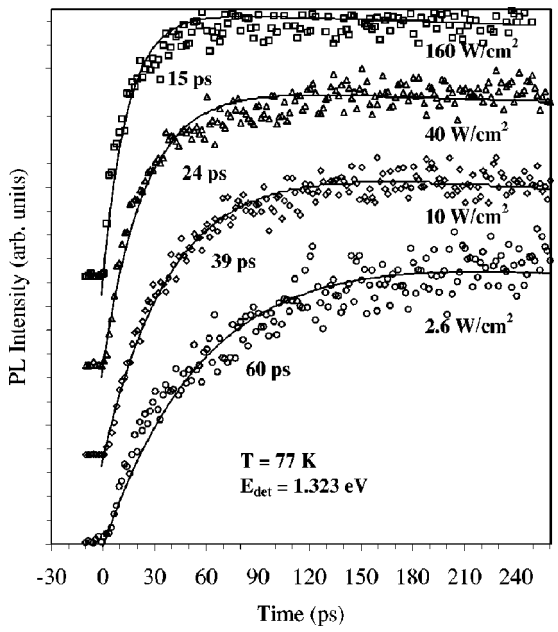

FIG. 9. Short-time PL transients obtained using a detection energy at the ground state of the (311)*B* QD emission under various excitation densities. PL rise times extracted from modeling of these transients are also shown.

energy QD's also contributes to this redshift.[18]

The observation of state filling[19] at such low-excitation densities in TRPL, along with the large intersublevel separation extracted from fits to the PL spectra (see Fig. 3) suggest that the population of the first excited state in PL is predominantly due to state filling rather than thermal activation of carriers from the QD ground state. Filling of the first excited state may be obscured by the overlapping WL emission at low temperatures ($T \leqslant 70$ K). The observed increase in intensity of the first excited state with increasing temperature would be expected to result from reduction of the effective dot population caused by thermal emission of carriers from some of the dots. Thermal population of excited-states may also contribute to the observed excited-state emission at high temperatures. Similar effects have been observed in low-density $In_xGa_{1-x}As/GaAs(100)$ QD's.[15,20]

Additional information on carrier relaxation times in these (311)*B* QD's is required in order to explain the more prominent WL peak in the (311)*B* PL spectrum at temperatures below 70 K. The capture time cannot be extracted directly from the WL PL decays due to state-filling effects. However information on the total transfer time (capture + intersublevel relaxation) can be deduced from the rise time of the ground-state QD transition. Figure 9 compares the QD PL transients obtained for different excitation densities. PL rise times obtained using a three-level model are also indicated in this figure. Carrier transfer times are found to gradually decrease as the excitation density increases. The same trend has also been observed for comparable (100) QD's[18,21] and for (100) QD's of different sizes.[22] This behavior is explained by Auger processes that become the dominant relaxation mechanism at high-carrier densities. It is interesting to note that the carrier transfer time obtained under low excitation density ($P = 2.6$ W/cm^2) is about a factor of 6 longer in (311)*B* QD's (≈ 60 ps) compared to the value previously obtained for (100) QD's of similar diameter and density (≈ 10 ps). The reduced transfer rate in (311)*B* QD's could be due to slower carrier capture into the QD confined states and/or slower intersublevel relaxation mechanisms within the QD's. However, the strong interdot coupling observed in temperature-dependent PL indicates a high-capture efficiency by the dots. Inhibited carrier mobility in the WL, observed for (100) QD's in low densities,[15] would not be expected to play a large role in (311)*B* QD structures due to the high dot densities. The longer carrier transfer time of (311)*B* QD's is therefore attributed to slower intersublevel relaxation at low-excitation densities. Differences in the carrier relaxation mechanisms at low-excitation densities are likely due to the differences in the energy and spacing of QD states in (311)*B* and (100) InGaAs/GaAs heterostructures.

The strong WL emission observed in the low-temperature ($T < 70$ K) cw PL spectrum from (311)*B* QD's most likely results from the combined effect of a shallower confining potential and longer intersublevel relaxation times compared to (100) QD's. The observed intensity dependence of the WL emission on temperature (see Fig. 7) suggests that WL states may be continuously populated via carrier thermal transfer from the QD excited states. This could occur even at low temperatures due to the overlap of WL and QD excited-state emission energies (see Fig. 8). This analysis does not rule out the possibility of a smaller capture efficiency in (311)*B* QD structures relative to (100) QD's, which may also contribute to the stronger WL emission observed in PL. This issue will be clarified by investigation of the PL rise time of the ground-state (311)*B* QD emission as a function of temperature.[15]

V. CONCLUSION

In conclusion, our results show strong radiative emission from small, high-density Stranski-Krastanow $In_xGa_{1-x}As/GaAs(311)B$ QD's of nominal indium mole

fraction $x=0.6$. Temperature-dependent PL measurements indicate a low-potential barrier between the QD's and the WL and reveal strong interaction between neighboring quantum dots. Time-resolved photoluminescence results show a longer carrier transfer time for (311)*B* QD's compared to (100) QD's of similar diameter and density. This may be ascribed to differing energies and level separations of quantum dot states that affect the carrier relaxation mechanisms at low-excitation densities. The strong emission from the InGaAs WL observed in the PL spectrum from (311)*B* QD structures is attributed to the combined effect of a shallower confining potential and longer intersublevel relaxation time compared to (100) QD's. These results highlight the importance of factors such as QD height, strain, and segregation effects in determining the electronic structures and relaxation mechanisms of self-assembled quantum dots of similar shapes and diameters.

ACKNOWLEDGMENTS

C.L. would like to thank A. Sikorski for assistance with TEM sample preparation and X.Z. Liao for useful discussions.

[1] R. Notzel, J. Temmyo, and T. Tamamura, Nature (London) **369**, 131 (1994).
[2] J. Temmyo, R. Notzel, and T. Tamamura, Appl. Phys. Lett. **71**, 1086 (1997).
[3] K. Nishi, T. Anan, A. Gomyo, S. Kohmoto, and S. Sugou, Appl. Phys. Lett. **70**, 3579 (1997).
[4] M. Kawabe, Y.J. Chun, S. Nakajima, and K. Akahane, Jpn. J. Appl. Phys., Part 1 **36**, 4078 (1997).
[5] C. Lobo and R. Leon, J. Appl. Phys. **83**, 4168 (1998).
[6] X.Z. Liao, J. Zou, D.J.H. Cockayne, R. Leon, and C. Lobo, Phys. Rev. Lett. **82**, 5148 (1999).
[7] J. Tersoff, Phys. Rev. Lett. **81**, 3183 (1998).
[8] N. Grandjean, J. Massies, and M. Leroux, Phys. Rev. B **53**, 998 (1996).
[9] R. Leon, S. Fafard, P.G. Piva, S. Ruvimov, and Z. Liliental-Weber, Phys. Rev. B **58**, R4262 (1998).
[10] R. Leon, S. Marcinkevičius, X.Z. Liao, J. Zou, D.J.H. Cockayne, and S. Fafard, Phys. Rev. B **60**, R8517 (1999).
[11] M. Ilg and K. Ploog, Phys. Rev. B **48**, 11 512 (1993).
[12] M. Ilg, M.I. Alonso, A. Lehmann, K. Ploog, and M. Hohenstein, J. Appl. Phys. **74**, 7188 (1993).
[13] K. Muraki, S. Fukatsu, Y. Shiraki, and R. Ito, Appl. Phys. Lett. **61**, 557 (1992).
[14] S. Paul, J.B. Roy, and P.K. Basu, J. Appl. Phys. **69**, 827 (1991).
[15] C. Lobo, R. Leon, S. Marcinkevičius, W. Yang, P.C. Sercel, X.Z. Liao, J. Zou, and D.J.H. Cockayne, Phys. Rev. B **60**, 16 647 (1999).
[16] R. Leon, Y. Kim, C. Jagadish, M. Gal, J. Zou, and D.J.H. Cockayne, Appl. Phys. Lett. **69**, 1888 (1996).
[17] R. Leon, D.R.M. Williams, J. Krueger, E.R. Weber, and M.R. Melloch, Phys. Rev. B **56**, R4336 (1997).
[18] S. Marcinkevičius and R. Leon, Phys. Rev. B **59**, 4630 (1999).
[19] S. Raymond, S. Fafard, P.J. Poole, A. Wojs, P. Hawrylak, S. Charbonneau, D. Leonard, R. Leon, P.M. Petroff, and J.L. Merz, Phys. Rev. B **54**, 11 548 (1996).
[20] C. Lobo (unpublished).
[21] N. Perret, D. Morris, and S. Fafard, in *Proceedings of the 194th Meeting of the Electrochemical Society, Fifth International Symposium on Quantum Confinement: Nanostructures* (Electrochemical Society, Boston, 1998).
[22] D. Morris, S. Fafard, and N. Perret, Appl. Phys. Lett. **75**, 3593 (1999).